AIP | Journal of Applied Physics

Donor ionization in size controlled silicon nanocrystals: The transition from defect passivation to free electron generation

I. F. Crowe, N. Papachristodoulou, M. P. Halsall, N. P. Hylton, O. Hulko et al.

Citation: J. Appl. Phys. **113**, 024304 (2013); doi: 10.1063/1.4772947
View online: http://dx.doi.org/10.1063/1.4772947
View Table of Contents: http://jap.aip.org/resource/1/JAPIAU/v113/i2
Published by the American Institute of Physics.

Donor ionization in size controlled silicon nanocrystals: The transition from defect passivation to free electron generation

I. F. Crowe,[1,a)] N. Papachristodoulou,[1] M. P. Halsall,[1] N. P. Hylton,[2] O. Hulko,[3] A. P. Knights,[3] P. Yang,[4] R. M. Gwilliam,[4] M. Shah,[5] and A. J. Kenyon[5]
[1]*Photon Science Institute, School of Electrical and Electronic Engineering, Alan Turing Building, University of Manchester, Manchester M13 9PL, United Kingdom*
[2]*Blackett Laboratory, Department of Physics, Imperial College London, London SW7 2AZ, United Kingdom*
[3]*Department of Engineering Physics and the Centre for Emerging Device Technologies, McMaster University, 1280 Main Street West, Hamilton, L8S 4L7 Ontario, Canada*
[4]*Surrey Ion Beam Centre, Advanced Technology Institute, University of Surrey, Guildford GU2 5XH, United Kingdom*
[5]*Department of Electronic and Electrical Engineering, University College London, London WC1E 7JE, United Kingdom*

(Received 12 June 2012; accepted 5 December 2012; published online 8 January 2013)

We studied the photoluminescence spectra of silicon and phosphorus co-implanted silica thin films on (100) silicon substrates as a function of isothermal annealing time. The rapid phase segregation, formation, and growth dynamics of intrinsic silicon nanocrystals are observed, in the first 600 s of rapid thermal processing, using dark field mode X-TEM. For short annealing times, when the nanocrystal size distribution exhibits a relatively small mean diameter, formation in the presence of phosphorus yields an increase in the luminescence intensity and a blue shift in the emission peak compared with intrinsic nanocrystals. As the mean size increases with annealing time, this enhancement rapidly diminishes and the peak energy shifts further to the red than the intrinsic nanocrystals. These results indicate the existence of competing pathways for the donor electron, which depends strongly on the nanocrystal size. In samples containing a large density of relatively small nanocrystals, the tendency of phosphorus to accumulate at the nanocrystal-oxide interface means that ionization results in a passivation of dangling bond (P_b-centre) type defects, through a charge compensation mechanism. As the size distribution evolves with isothermal annealing, the density of large nanocrystals increases at the expense of smaller nanocrystals, through an *Ostwald* ripening mechanism, and the majority of phosphorus atoms occupy substitutional lattice sites within the nanocrystals. As a consequence of the smaller band-gap, ionization of phosphorus donors at these sites increases the free carrier concentration and opens up an efficient, non-radiative de-excitation route for photo-generated electrons via *Auger* recombination. This effect is exacerbated by an enhanced diffusion in phosphorus doped glasses, which accelerates silicon nanocrystal growth.
 [http://dx.doi.org/10.1063/1.4772947]

I. INTRODUCTION

Silicon nanocrystals have a promising future in silicon photonics because the spatial confinement of the electron and hole wave-functions significantly improves the radiative transition probability compared with bulk silicon.[1] One area of particular interest is the specific interaction of silicon nanocrystals with donor and/or acceptor impurities, most notably phosphorus and boron.[2,3] Recent work has shown that phosphorus doping can result in either a quenching or an enhancement of the silicon nanocrystal photoluminescence,[1,4,5] dependent on the dopant concentration and the specific sample preparation. If future device applications are to include silicon nanocrystal based materials, it is evident that a degree of control over the optical and electronic properties of *p*- or *n*-type structures must be realised. Understanding the luminescence process in the presence of phosphorus relies on determining the precise nature of the interaction between the nanocrystals and the dopant ions. In this contribution, we present an investigation into the effect of phosphorus ion implant doping on the luminescence associated with silicon nanocrystals as a function of the specific annealing environment. We demonstrate, in particular that, for fixed silicon excess and phosphorus concentrations, the isothermal annealing time is critical in observing either a quenching or enhancement in the luminescence intensity and offer an explanation for this, based on the interaction of phosphorus dopants with different size silicon nanocrystals.

II. EXPERIMENTAL DETAILS

A. Sample preparation

A 500 nm SiO_2 film was grown by "wet" thermal oxidation from single crystal (100) Si. The oxide films were then implanted with Si^+ at 80 keV to an areal density of 8×10^{16} at/cm^2, which yields a distribution of excess silicon atoms in a ~100 nm wide band, centered ~100 nm below the surface, as predicted by *Monte Carlo* simulations using the Stopping and Range of Ions in Matter (SRIM 2003) software and verified by

[a)]Author to whom correspondence should be addressed. E-mail: iain.crowe@manchester.ac.uk.

TEM (not shown here). The implanted distribution yields a peak concentration of ~10 at. % excess silicon, as verified by *Rutherford* backscattering spectroscopy (not shown here). Half of the wafer was also implanted with P^+ at 80 keV to 5×10^{15} at/cm^2, which yields a similar implant profile but with a peak phosphorus concentration of ~0.8 at. %. Annealing of the silicon supersaturated oxide films to obtain nanocrystals and to remove implantation damage was executed using a commercial *Jipelec Jetfirst* 100 rapid thermal processor in a nitrogen (N_2) ambient for isothermal (1050 °C) anneal times in the range 1 to 600 s. All samples were post-process annealed in a mixed N_2:H_2(5%) forming gas at 500 °C for a further 5 min, which is known to passivate the so-called "dangling-bond" type interfacial defects (P_b-centres).[6]

B. Cross-sectional transmission electron microscopy (X-TEM)

Structural characterization of the samples was performed by X-TEM using a Philips CM-12 operated at 120 kV. Cross-sectional specimens oriented along the {110} zone axis were prepared by standard mechanical polishing, followed by ion milling. Dark-field examinations were carried out with two beam diffraction condition (g = 220) relative to the silicon substrate (rather than using the polycrystalline ring from the nanocrystals) in order to compare the size (and depth) distribution for all analyzed samples. Whilst the random orientation of the nanocrystals naturally yields an underestimate for the absolute density using this technique, the *relative* density, size, and distribution of nanocrystals in the implanted layer as a function of annealing time can be determined in a highly repeatable manner. Our experimental observation showed that the amount of observable nanocrystals depends on the chosen segment of the poly-ring and varies from ~10% to 15% of the total population (15% using 220 diffraction conditions). For each sample, several high magnification (125 and 200 k) images were also taken in sequence, accounting for the entire nanocrystal distribution, and from which the nanocrystal sizes could be more accurately measured.

C. Photoluminescence (PL) spectroscopy

Photo-excitation was provided by a 405 nm, 15 mW laser diode, focussed using a 40 × microscope objective lens. The PL was collected confocally and measured using a *Bayspec* fiber coupled spectrometer with an integrated, thermoelectrically cooled charge coupled device array. All measurements were conducted at room temperature and the spectra were corrected for the system response. For the time resolved PL, photo-excitation was provided by a Diode Pumped Solid State (DPSS) laser emitting at 473 nm. The laser beam was steered through a prism and diaphragm in order to remove unwanted wavelengths and modulated using a *Pockels* cell at a frequency of 2.5 KHz. The PL transients were detected using a Near Infra-Red (NIR)-sensitive *Hamamatsu* photomultiplier tube (R5509-72) and recorded with a digital storage oscilloscope.

III. RESULTS AND DISCUSSION

Figure 1 shows the evolution of the (intrinsic) silicon nanocrystal size distribution with isothermal annealing time.

As the annealing time increases, the rapid formation of clusters is followed by an increase in their mean size and a corresponding reduction in their relative density. This phenomenon is characteristic of *Ostwald* ripening after the phase segregation of a meta-stable alloy.[7,8] For a fixed concentration and annealing temperature, the homogeneous growth of the clusters is primarily limited by ion diffusion in the host matrix.[9,10] However, it is well known that the formation energy can be lowered significantly, and the rate of cluster growth enhanced at pre-existing defect, or impurity sites, via heterogeneous growth.[8]

The samples prepared for this study exhibit PL spectra typical of silicon nanocrystals,[4,11] Figure 2 with a broad peak centred close to 1.5 eV (800 nm).

The peak of the emission band is monotonously red-shifted with increasing anneal time, indicative of a reduction in the recombination energy as the mean size of the nanocrystals increases, in accordance with a quantum confinement model. We note, however, that the shift in emission for

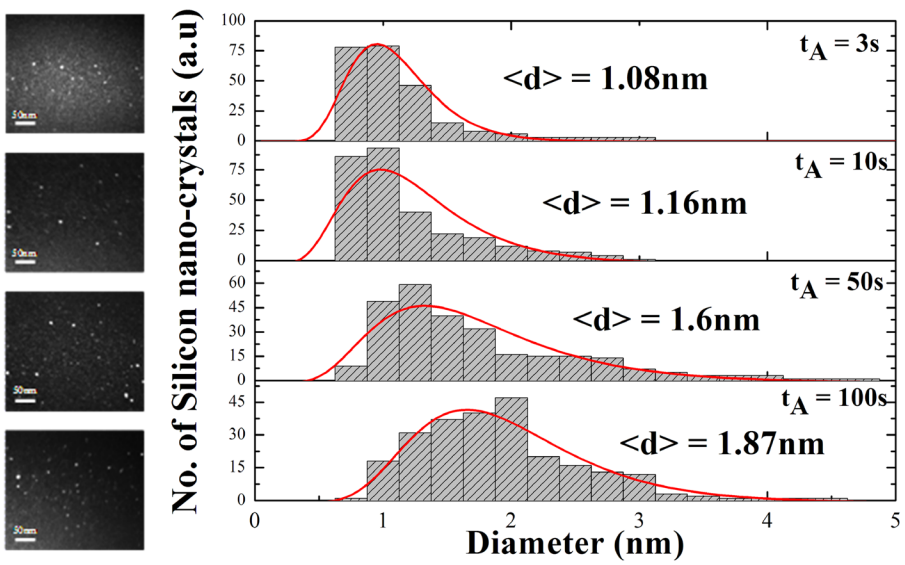

FIG. 1. (Left) Dark-field X-TEM images and (right) histogram showing the evolution of the intrinsic ([P] = 0) silicon nanocrystal ensemble size distribution with increasing isothermal (1050 °C) anneal time, t_A in the range 3 to 100 s. The red lines are lognormal fits to the data, which provides the mean nanocrystal size, ⟨d⟩.

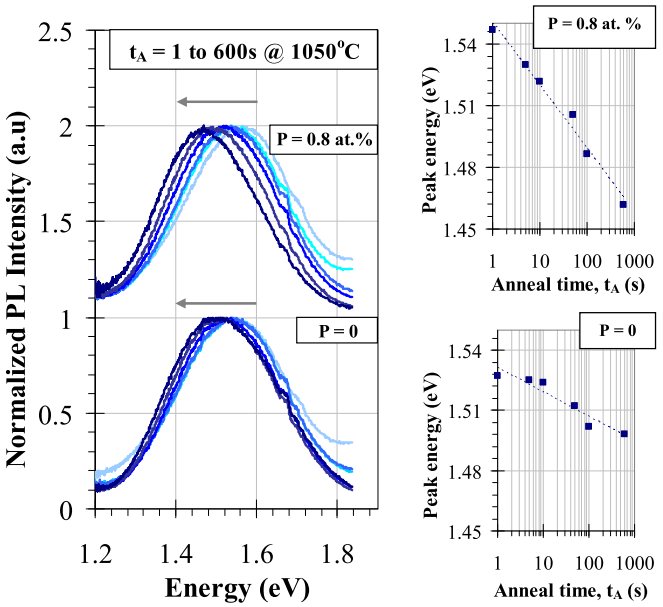

FIG. 2. (Left) Normalized room temperature PL spectra (offset for clarity) and (right) PL peak emission energy for (bottom) intrinsic and (top) phosphorus doped silicon nanocrystals as a function of isothermal (1050 °C) anneal time (t_A = 1, 5, 10, 50, 100, and 600 s).

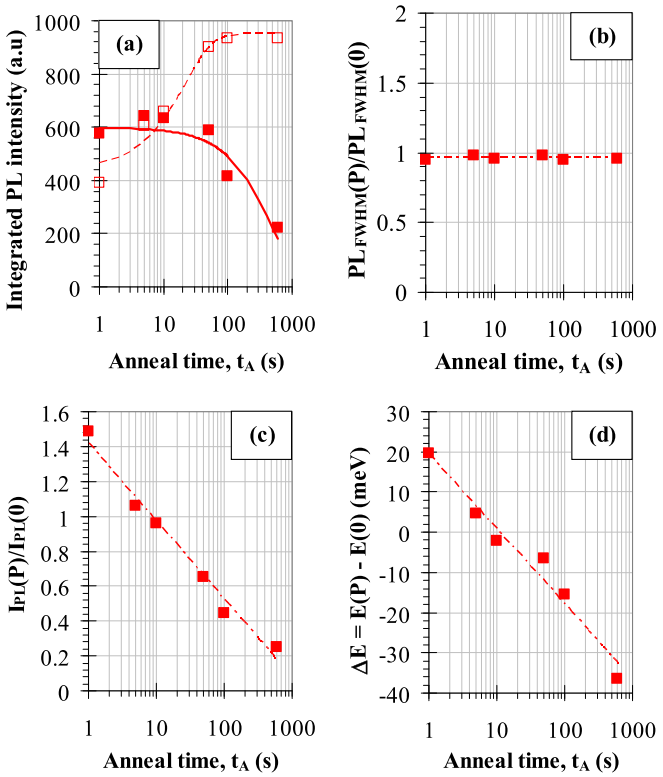

FIG. 3. (a) Integrated PL intensity for the intrinsic (open squares) and phosphorus doped (closed squares) silicon nanocrystals as a function of the isothermal (1050 °C) anneal time, (b), (c), and (d), respectively, show the evolution of the ratios of the PL full width at half maximum, $PL_{FWHM}(P)/PL_{FWHM}(0)$, integrated PL intensities, $I_{PL}(P)/I_{PL}(0)$ and the difference in peak emission energy, $\Delta E = E(P) - E(0)$ over the annealing time range. Lines are to guide the eye.

the phosphorus doped samples, over this range of annealing times, is ~3 times larger than for the intrinsic nanocrystals. This suggests that the growth is accelerated when formation takes place in the presence of phosphorus. It is well known that phosphorus doped glasses "soften" at much lower temperatures than un-doped SiO_2 matrices because of Si-O-Si bond substitution with hydroxyl radicals, for example Si-O-POH, which increases the open volume density.[12] This lowers the melting temperature[13] and increases the thermal expansion coefficient relative to pure silica glass and can result in an increased ion diffusion length.[14] For the silicon rich oxide system this likely leads to an accelerated segregation of the Si and SiO_2 phases.[15] The re-crystallization of bulk silicon is also known to be accelerated following amorphization via high dose phosphorus ion irradiation.[16] Previous microscopy studies, in which the silicon nanocrystal size was observed to increase with phosphorus doping,[17] further support this hypothesis.

Figure 3 shows the ratio of integrated intensities, $I_{PL}(P)/I_{PL}(0)$, and the absolute difference in the peak emission energy, $\Delta E = E(P) - E(0)$, for the phosphorus doped and intrinsic nanocrystal emission, as a function of the isothermal anneal time.

For the shortest anneal time ($t_A = 1$ s), when the size distribution exhibits the smallest mean diameter and largest density of relatively small nanocrystals, formation in the presence of phosphorus results in a ~50% higher integrated luminescence intensity and an emission peak that is blue-shifted by ~20 meV compared with the intrinsic nanocrystals. However, as the anneal time increases, the PL enhancement is rapidly quenched and the blue-shift disappears until, at $t_A = 600$ s, the emission intensity of the phosphorus doped nanocrystals is a factor ~5 smaller and almost 40 meV to the "red" side of the intrinsic nanocrystal peak. Similar results were reported by Tchebotareva *et al.*[18] when investigating the effect of increasing phosphorus concentration on silicon nanocrystal luminescence, also in films prepared by ion implantation.

Previous studies[6,7] have shown that initial formation of the nanocrystal interface necessarily produces a high density of dangling bond (P_b-centre) type defects, which are thought to be the most likely non-radiative recombination centre for photo-excited carriers in these films. The presence of phosphorus atoms in the matrix probably mediates this interface formation by acting as a "seed" centre, which encourages heterogeneous nucleation. If the nanocrystal formation sites strongly correlate with the position of the (phosphorus) impurity centres, as might be expected when the implant profiles of the two species are well aligned, then dangling bond formation might be suppressed via charge compensation, as previously evidenced by electron paramagnetic resonance studies.[19] This would reduce the density of non-radiative defects and give rise to an increase in the contribution to the luminescence,[20,21] particularly for smaller nanocrystals in the ensemble population because of their higher surface to volume ratio. We reject the hypothesis that the luminescence enhancement for the phosphorus doped nanocrystals comes from an increase in the radiative transition rate, $w_R = 1/\tau_R$ as previously suggested,[22] because the total PL decay rate, $w_{PL} = w_{NR} + w_R$ we have measured, Figure 4 is smaller for the phosphorus doped nanocrystals at short anneal times (where the PL enhancement is observed). Rather, we propose

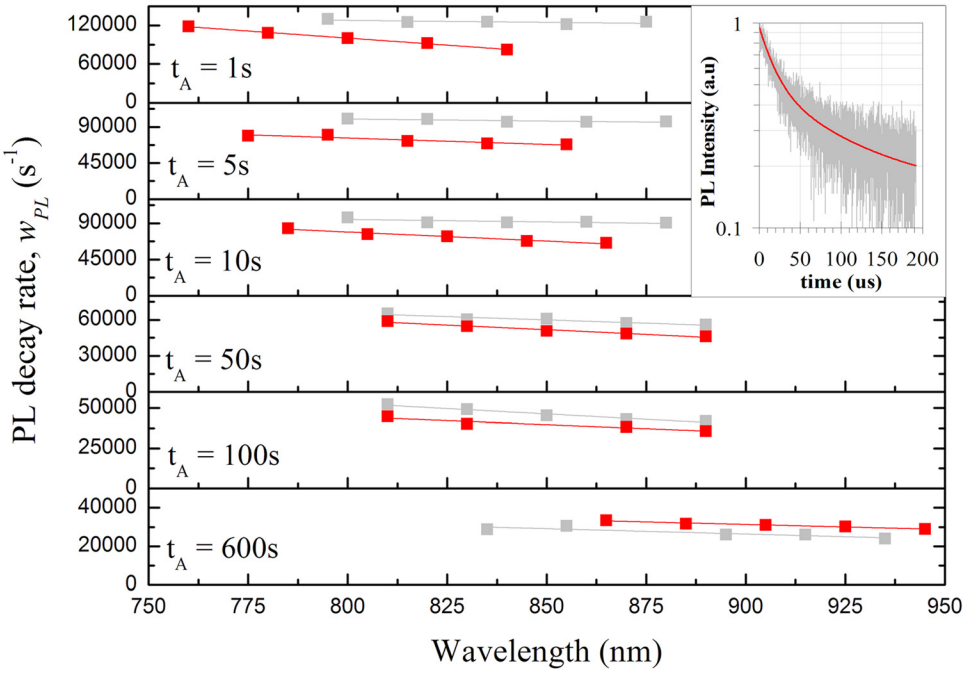

FIG. 4. Evolution of the spectrally resolved PL decay rates for the phosphorus doped (red squares) and intrinsic (grey squares) silicon nanocrystals as a function of isothermal (1050 °C) anneal time. The inset shows a typical PL decay curve, the fit (red line) of which is derived from a stretched exponential function, $I(t) = e^{\left(-\frac{t}{\tau_{PL}}\right)^{\beta}}$ giving characteristic lifetimes, $\tau_{PL} = w_{PL}^{-1}$.

that, as $w_{NR} \gg w_R$, a decrease in the measured decay rate (increase in the measured lifetime) for the phosphorus doped silicon nanocrystals most likely indicates a smaller contribution of w_{NR} (lower defect density) to the total decay rate.

As for the larger nanocrystals, whose density and crystalline fraction both increase with anneal time, the probability that phosphorus atoms occupy substitutional lattice sites also increases. As a consequence of their smaller band-gap, ionization of these substitutional donors results in an increase in the free carrier concentration.[14,19] This opens up an efficient, non-radiative de-excitation channel for photogenerated electrons via *Auger* recombination, which would dramatically reduce radiative efficiency, evidenced here by a quenching of the luminescence signal at long t_A, relative to that of the intrinsic nanocrystals. Similar observations to these were reported when varying the phosphorus concentration for a fixed nanocrystal size distribution.[4,23]

The specific observation here of a transition from defect passivation to free carrier generation implies a "threshold size" for dopant activation in silicon (and likely other) nanocrystal materials. It is possible to obtain a rudimentary estimate of this "threshold size" by combining the X-TEM data we have taken for the intrinsic nanocrystals and that of Hao *et al.*[17] in which the phosphorus induced size increase was measured for a range of annealing temperatures. Although the sample preparation in Ref. 17 is different to that described in the present study, similar concentrations of both phosphorus and silicon were used, which we believe is the most important factor in determining the structural and optoelectronic properties of the films. According to the data in Ref. 17, annealing phosphorus doped films for 1 h at 1000 °C yields nanocrystals that are ~12.5% larger than their intrinsic counterparts. At 1100 °C, this figure increases to ~90%, and, although no data are available for the annealing temperature we have employed here (1050 °C), interpolation of the data in Ref. 17 between 1000 and 1100 °C reveals this to be ~52%. Figure 5 illustrates how this would affect the evolution of intrinsic nanocrystals over the annealing time range we have employed.

An estimate of the "threshold size," $d_{threshold} \sim 1.85$ nm, above which the majority of nanocrystals in the ensemble contain free carriers after the ionization of substitutional phosphorus donors, agrees remarkably well with previous theoretical predictions.[24] In that work, the authors showed that, for silicon nanocrystals smaller than about 2 nm, phosphorus atoms will always be energetically expelled towards the surface during formation.

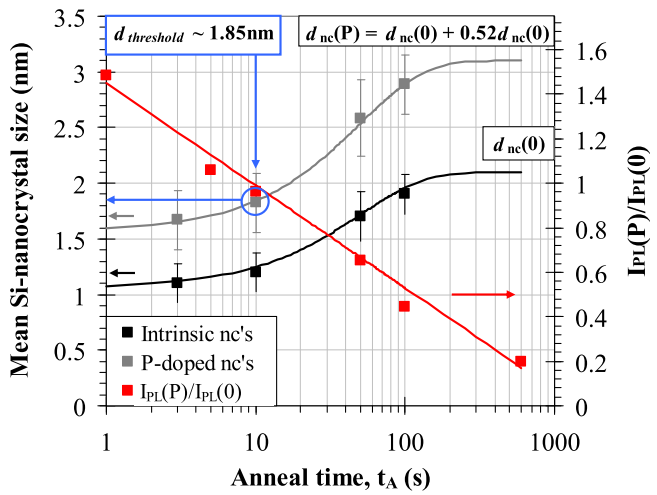

FIG. 5. (Left axis) Evolution of the measured intrinsic (black squares) nanocrystal mean diameter and that estimated (for a 52% size increase) for the phosphorus doped (grey squares) nanocrystals. (Right axis) Ratio of the integrated PL intensities, $I_{PL}(P)/I_{PL}(0)$ (red squares) as a function of the isothermal (1050 °C) anneal time. The blue arrows and circle indicate the nanocrystal size at which $I_{PL}(P)/I_{PL}(0) = 1$ and therefore provides an estimate of the "threshold size" ($d_{threshold} \sim 1.85$ nm) above which the majority of nanocrystals contain free carriers after the ionization of substitutional phosphorus donors.

IV. CONCLUSIONS

By studying the effect of isothermal annealing time on the luminescence spectra for intrinsic and phosphorus doped silicon nanocrystals, we have been able to observe a transition from defect passivation to free carrier generation as the nanocrystal size distribution evolves. Our observations strongly support the hypothesis that, at short anneal times, the phosphorus performs a passivating function for the smallest nanocrystals in the ensemble as evidenced by an enhancement of the integrated intensity and corresponding blue-shift of the emission peak. This is likely mediated by a charge compensation of silicon dangling bonds by phosphorus donors. As the anneal time increases, however, the fraction of nanocrystals containing ionized phosphorus donors at substitutional lattice sites increases and the luminescence enhancement rapidly diminishes. This is due to the onset of an efficient non-radiative de-excitation pathway for photo-excited electrons, likely mediated via *Auger* recombination on account of the larger free electron concentration. These data indicate the existence of a "threshold size," $d_{threshold}$ below which the ionization of phosphorus donors primarily contributes to charge compensation of dangling bond interface defects and above which they contribute to an increase in the free carrier concentration. We estimate, from available TEM data and the ratio of integrated luminescence intensities of phosphorus doped to intrinsic silicon nanocrystals, that $d_{threshold} \sim 1.85\,\text{nm}$, which is in very good agreement with previous theoretical models. This information is likely to be equally valuable in optimizing luminescence efficiency of future silicon photonic materials and in understanding the donor activation in materials for future nano-electronic devices.

[1]V. A. Belyakov, V. A. Burdov, R. Lockwood, and A. Meldrum, Adv. Opt. Tech. **2008**, 279502 (2008).
[2]M. Fujii, Y. Yamaguchi, Y. Takase, K. Ninomiya, and S. Hayashi, Appl. Phys. Lett. **87**, 211919 (2005).
[3]S. Ossicini, F. Iori, E. Degoli, E. Luppi, R. Margi, G. Cantele, F. Trani, and D. Ninno, in *2nd IEEE International Conference on Group IV Photonics* (IEEE, 2005), p. 60.
[4]A. P. Knights, J. N. Milgrarn, J. Wojcik, P. Mascher, I. Crowe, B. Sherliker, M. P. Halsall, and R. M. Gwilliam, Phys. Status Solidi A **206**, 969 (2009).
[5]M. Fujii, A. Mimura, S. Hayashi, D. Kovalev, and F. Koch, Phys. Rev. B **62**, 12625 (2000).
[6]P. Pellegrino, B. Garrido, C. García, R. Ferré, J. A. Moreno, and J. R. Morante, Phys. E **16**, 424 (2003).
[7]B. G. Fernandez, M. Lopez, C. Garcia, A. Perez-Rodriguez, J. R. Morante, C. Bonafos, M. Carrada, and A. Claverie, J. Appl. Phys. **91**, 798 (2002).
[8]D. A. Porter and K. E. Easterling, *Phase Transformations in Metals and Alloys* (Chapman and Hall, London, 1992).
[9]A. Podhorodecki, G. Zatryb, J. Misiewicz, J. Wojcik, and P. Mascher, J. Appl. Phys. **102**, 043104 (2007).
[10]G. A. Kachurin, K. S. Zhuravlev, N. A. Pazdnikov, A. F. Leier, I. E. Tyschenko, V. A. Volodin, W. Skorupa, and R. A. Yankov, Nucl. Instrum. Methods Phys. Res. B **127–128**, 583 (1997).
[11]J. H. Shim and N. H. Cho, Glass Phys. Chem. **31**, 525 (2005).
[12]S. Prakash, W. E. Mustain, S. Park, and P. A. Kohl, J. Power Sources **175**, 91 (2008).
[13]N. I. Belyusenko and Y. P. Kareev, Glass Ceram. **36**, 206 (1979).
[14]K. Sumida, K. Ninomiya, M. Fujii, K. Fujio, S. Hayashi, M. Kodama, and H. Ohta, J. Appl. Phys. **101**, 033504 (2007).
[15]M. Fujii, Y. Yamaguchi, Y. Takase, K. Ninomiya, and S. Hayashi, Appl. Phys. Lett. **85**, 1158 (2004).
[16]D. Tetelbaum and A. Gerasimov, Semiconductors **38**, 1260 (2004).
[17]X. J. Hao *et al.*, Thin Solid Films **517**, 5646 (2009).
[18]A. L. Tchebotareva, M. J. A. de Dood, J. S. Biteen, H. A. Atwater, and A. Polman, J. Lumin. **114**, 137 (2005).
[19]A. R. Stegner, R. N. Pereira, K. Klein, H. Wiggers, M. S. Brandt, and M. Stutzmann, Physica B **401–402**, 541 (2007).
[20]M. Fujii, A. Mimura, S. Hayashi, and K. Yamamoto, Appl. Phys. Lett. **75**, 184 (1999).
[21]M. Fujii, A. Mimura, S. Hayashi, K. Yamamoto, C. Urakawa, and H. Ohta, J. Appl. Phys. **87**, 1855 (2000).
[22]V. A. Belyakov and V. A. Burdov, Phys. Rev. B **79**, 35302 (2009).
[23]X. D. Pi, R. Gresback, R. W. Liptak, S. A. Campbell, and U. Kortshagen, Appl. Phys. Lett. **92**, 123102 (2008).
[24]T. L. Chan, M. L. Tiago, E. Kaxiras, and J. R. Chelikowsky, Nano Lett. **8**, 596 (2008).